CHEMISTRY of MATERIALS

VOLUME 10, NUMBER 6 JUNE 1998

Communications

Reworkable Epoxies: Thermosets with Thermally Cleavable Groups for Controlled Network Breakdown

Shu Yang, Jir-Shyr Chen, Hilmar Körner, Thomas Breiner, and Christopher K. Ober*

Department of Materials Science and Engineering, Bard Hall, Cornell University, Ithaca, New York 14853-1501

Mark D. Poliks

IBM Microelectronics, Endicott, New York 13760

Received October 7, 1997
Revised Manuscript Received March 26, 1998

Introduction

The very good thermal stability of polymer thermosets has produced the need for materials with reworkable behavior, that is, materials whose mechanical properties can be degraded under controlled circumstances. Rework enables the straightforward repair, replacement, recycling, or short-term use of structures assembled with such materials. It is well-known that lower modulus thermoplastic polymers can be easily removed by an appropriate choice of solvent or heat. However, in many applications thermosets are the materials of choice for long-term use because they are insoluble, infusible high-density networks.[1−4] Conventional thermosets are difficult or impossible to thoroughly remove without damaging underlying structures. Recycling is thus also difficult.

If the chemical, physical, and mechanical properties of a thermoset network can be adjusted in a controlled way, rework of thermosets can take place. Little prior research has been carried out on this topic due to the complicated nature of the chemical structure of both thermosets and hardeners, curing kinetics and mechanisms, and the network structure of thermosets. Most reports have focused on the effect of physical and thermal aging of conventional thermosets. Recently work has been done on the molecular level design of reworkable thermosets using a variety of approaches.[5−7] Sastri and Tesoro[5] have investigated thermosets with disulfide-containing cross-linking agents, which introduce a cleavable linkage in the hardener. The thermoset can be easily ruptured after reducing the cross-link density. The method developed by Hall et al.[6] was to mix low melting point thermoplastics with conventional thermosets. At a desired temperature, the thermoplastic melts and the system softens and drops to very low modulus, thus permitting rework. Another approach pioneered by Buchwalter[7] has been to design a latent weak linkage (e.g., acetal/ketal groups) in the thermoset network to be disconnected under controlled conditions, such as soaking of the thermosets in a dilute acid solution.

In this paper, we report the synthesis and characterization of a series of new epoxy compounds that incorporate thermally cleavable groups. Two criteria were

(1) Manzione, L. T. *Plastic Packaging of Microelectronic Devices*; Van Nostrand Reinhold: New York, 1990.
(2) Stevens, J. J. In *Epoxy Resin Technology*; Bruins, P. F., Ed.; Interscience Publishers: New York, 1968; p 11.
(3) Robock, P. V.; Nguyen, L. T. In *Microelectronics Packaging Handbook*, Tummala, R. R., Rymaszewski, E. J., Eds.; Van Nostrand Reinhold: New York, 1989; p 523.
(4) Lau, J. H. In *Chip on Board Technologies for Multichip Modules*; Van Nostrand Reinhold: New York, 1994.
(5) (a) Licari, J. J.; Bakhit, G. G. U.S. Patent 5,002,818. (b) Sastri, V. R.; Tesoro, G. C. *J. Appl. Polym. Sci.* **1990**, *39*, 1425−1437. (c) Sastri, V. R.; Tesoro, G. C. *J. Appl. Polym. Sci.* **1990**, *39*, 1439−1457.
(6) Hall, J. B.; Hogerton, P. B.; Pujol, J. M. U.S. Patent 5,457,149.
(7) (a) Buchwalter, S. L.; Kosbar, L. L. *J. Polym. Sci. Part A: Polym. Chem.* **1996**, *34*, 249−260. (b) Afzali-Ardakani, A.; Buchwalter, S. L.; Gelorme, J. D.; Kosbar, L. L.; Pompeo, F. L. U.S. Patent 5,512,613.

S0897-4756(97)00667-4 CCC: $15.00
Published on Web 05/15/1998

identified for the design of this new type of reworkable epoxy. First, the new epoxy should retain the room-temperature liquid characteristics of previously used cycloaliphatic epoxy thermosets, while at the same time the network backbone should be cleaved in a controlled way by either heat or solvent. Second, the new epoxy should not decompose during the curing reaction.

On the basis of the known thermal decomposition mechanisms of esters,[8] secondary and tertiary esters were identified as potential heat-cleavable linking groups that can decompose with or without added acid. Such esters may be either formed during the curing reaction or introduced as distinct groups in the epoxy resin. On the basis of this premise, we synthesized several new epoxies that either (i) contain secondary or tertiary esters linking the epoxy groups or (ii) establish tertiary ester bonds during the curing reaction. These chemical groups were chosen to decompose between 200 and 300 °C. This report describes the reworkable nature of such thermosets using decomposition controlled by local heating. The thermochemical and thermomechanical stability of the resulting cured thermosets was also investigated. These thermosets are shown to retain the mechanical properties of compositionally similar conventional thermosets at room temperature while exhibiting large differences above the glass transition temperature.

Results and Discussion

Several new diepoxy compounds with either secondary or tertiary ester links were synthesized (see Figure 1). The epoxy *sec*-epoxide (**5a**) was produced with a secondary ester linkage, while the following three epoxies contain tertiary esters: (i) *tert*-epoxide (**5b**), (ii) α-*terp*-epoxide (**5c**), and (iii) *sym*-α-*terp*-epoxide (**5d**). Details of the ^{1}H NMR and FT-IR data for these compounds are given in the Experimental Section. These epoxies were compared with the commercially available primary ester epoxy, Union Carbide ERL-4221 (**5e**) resin, to examine the effect of a tertiary ester linkage on network performance. After curing with anhydride, the epoxy **5e** formed a polyester network with both primary and secondary ester groups, in contrast to the tertiary ester bonds present in the new thermosets (see Figure 2). The tertiary ester links could be thermally broken down at lower temperatures than required for epoxy **5e** with primary and secondary ester groups. In addition, both the α-*terp*-epoxide (**5c**) and *sym*-α-*terp*-epoxide (**5b**) had a methyl group on the epoxy ring, resulting in additional tertiary esters at the cross-link sites after anhydride curing. Later in this paper, we discuss the results of TGA and FT-IR measurements with different ester linkages and the effect of the number of tertiary ester links per cross-link site.

Curing Reaction. Generally, cycloaliphatic resins are cured by acids or acid anhydrides to give high cross-link density resins. Amines were not used because of their low reactivity: at high curing temperatures, the possible aminolysis of the ester linkage must be avoided. In addition, the presence of base interferes with the autocatalytic thermal cleavage of esters by liberated protons. Following established curing procedures,[9] hexahydro-4-methylphthalic anhydride (HHMPA) and excess epoxide were mixed in a 0.87:1 mole ratio to avoid side reactions, such as etherification. By design, the epoxies have weak, acid-labile ester linkages between two epoxy functional groups, so it is important to lessen side reactions which may introduce acid groups that can cleave the secondary or tertiary ester bonds before the epoxy is fully cured. HHMPA is easier to work with than *cis*-1,2-cyclohexanedicarboxylic anhydride (HHPA) since HHMPA is a room-temperature liquid, while HHPA is a solid and mixes less homogeneously with each epoxy. Both HHPA and HHMPA are hygroscopic and can be hydrolyzed to the diacid. Once water is absorbed, the diacid formed may initiate decomposition at high temperatures. From both DSC and TGA data, it was observed that the specific ester linkage had little effect on curing behavior, since it was located far from the epoxy ring, while the methyl group on the epoxy ring did have a steric effect on curing. The ester bond was not cleaved during curing, and TGA data obtained at several heating rates and different temperatures showed that the thermal behaviors of thermosets cured by either HHMPA or HHPA were almost identical.

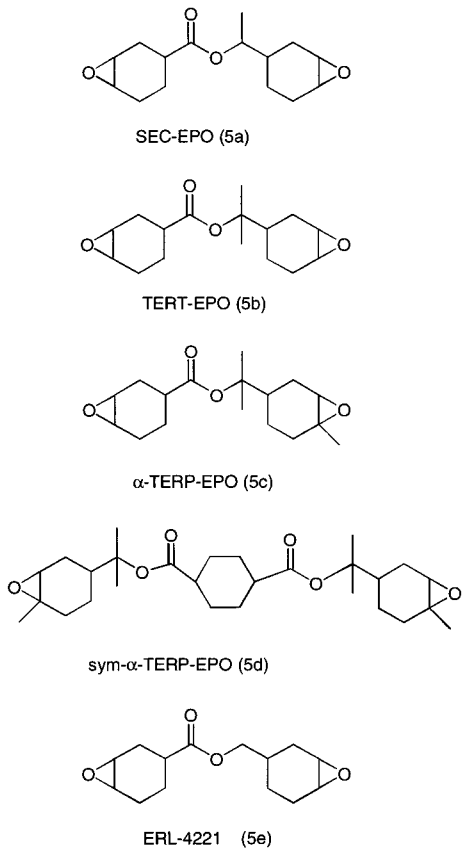

Figure 1. Chemical structures of cycloaliphatic epoxides.

Time-resolved FT-IR proved to be a very useful tool to study curing reaction kinetics.[10,11] As the curing reaction proceeded, the acid anhydride reacted with the

(8) Grassie, N.; Scott, G. *Polymer Degradation & Stabilisation*; Cambridge University Press: Cambridge, 1985.

(9) Buchwalter, S. L. *Polym. Prepr. (Am. Chem. Soc., Div. Polym. Chem.)* **1996**, *37* (1), 186.

(10) Körner, H.; Shiota, A.; Ober, C. K.; Laus, M. *Chem. Mater.* **1997**, *9*, 1588.

(11) (a) Antoon, M. K.; Koenig, J. L. *J. Polym. Sci.: Polym. Chem. Ed.* **1981**, *19*, 549. (b) Mertzel, E.; Koenig, J. L. *Adv. Polym. Sci.* **1986**, *75*, 74.

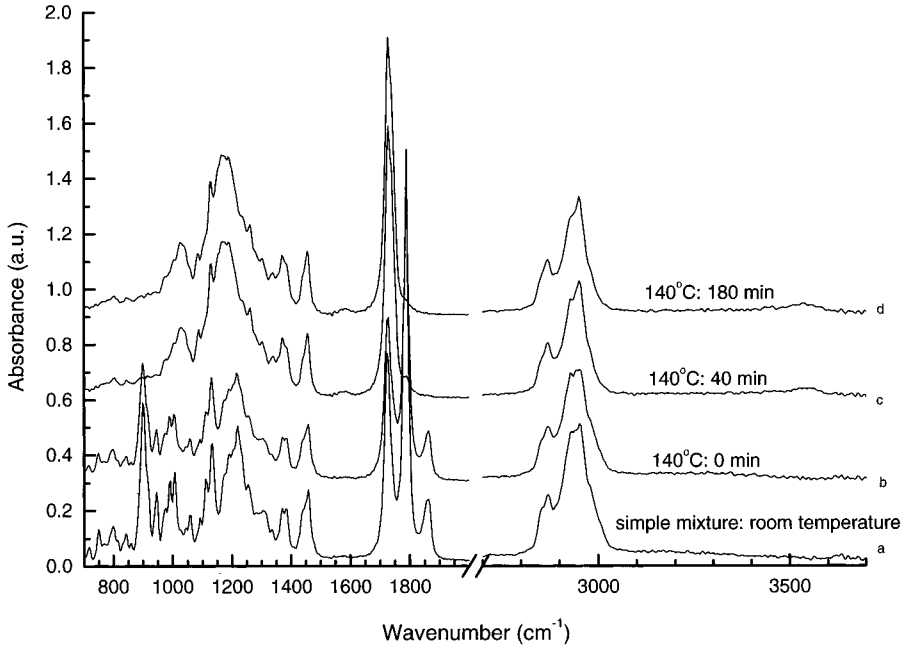

Figure 2. Time-resolved FT-IR of the α-terp-epoxide (**5c**)/HHMPA curing reaction at 140 °C, a−d.

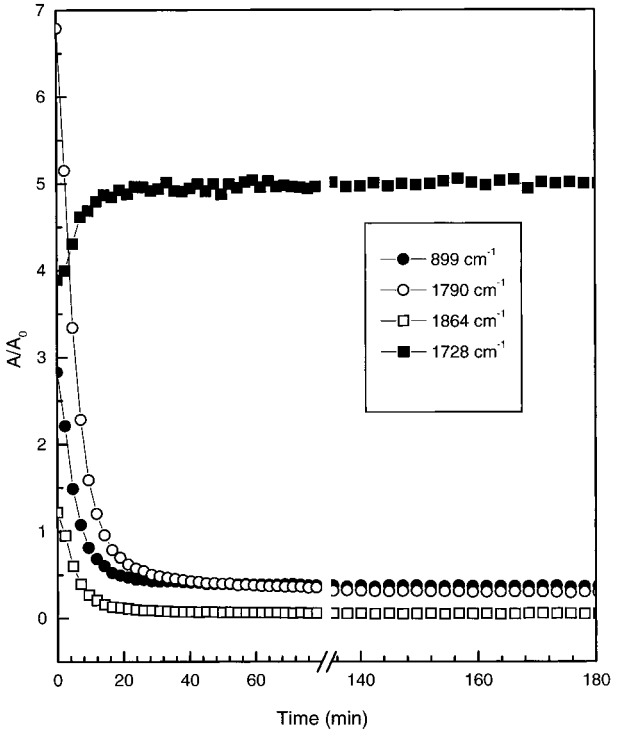

Figure 3. Normalized FT-IR absorbance of the α-terp-epoxide(**5c**)/HHMPA curing reaction at 140 °C vs time at selected wavenumbers.

epoxy function, and the ester bond was formed (see Figure 2). The curing process was easily monitored by a decrease in absorbance at 1864 and 1790 cm^{-1} (HHMPA acid anhydride C═O stretching) and at 899 cm^{-1} (epoxy C−O−C ring deformation) and by the corresponding increase of the absorbance at 1728−1730 cm^{-1} (ester C═O). The absorbance at 1377 cm^{-1} (C−H stretching of CH_3) was used as an internal standard to normalize the baseline and film thickness change of the samples during reaction. As shown in Figure 3, at 140 °C the curing reaction of **5c**/HHMPA was monitored as the change of absorbance of the peak of interest, *A*, over the reference absorbance at 1377 cm^{-1}, A_0, with time. Although each monitored peak had its own sensitivity, they all initially showed first order behavior. After 50 min, absorbance did not change, indicating that the reaction had become diffusion controlled due to the low mobility of functional groups. These results are comparable to those obtained from isothermal DSC at the same temperature.

Thermal Properties. As mentioned above, a goal of this research was to design a selected epoxy thermoset that incorporated thermally labile groups that disconnect if heated to a specific temperature. Using TGA and time-resolved FT-IR, the thermal decomposition behavior of these thermosets was studied. As seen from Figure 4, when heated at the same heating rate (10 °C/min), the thermosets from the tertiary epoxide (**5b**), the α-*terp*-epoxide (**5c**), and the *sym*-α-*terp*-epoxide (**5d**) started to lose weight at ∼220 °C, and those from the secondary epoxide (**5a**) started to decompose at ∼320 °C, whereas cured epoxy **5e** began to decompose at ∼340 °C. In the ester network, there are several different ester bonds with different bond strengths. At low temperature, weaker tertiary ester linkages of the reworkable thermosets are initially broken, followed by other decomposition chemistry at higher temperature. Data from MOPAC calculations are consistent with experimental observations and show that the ester (C−O) bond energies for both tertiary ester-containing epoxides **5b** and **5c** were much less (75.9 and 76.4 kcal/mol, respectively) than those for either the secondary **5a** (88.5 kcal/mol) or the primary ester (**5e**) epoxy (89.7 kcal/mol). Thermosets from **5b**, **5c**, and **5d** all have tertiary ester linkages in the network and show similar decomposition onset temperatures.

Compounds **5c** and **5d** have methyl groups on the epoxides (as noted previously), and we would expect some difference in their decomposition behavior due to the methyl group. When acid anhydride hardener opens the epoxy ring, a new tertiary ester is formed to create additional decomposable units in the network. We

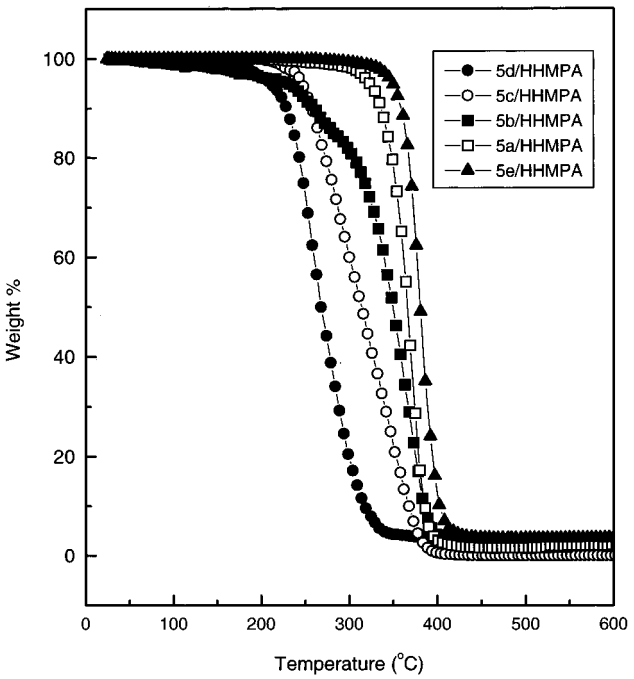

Figure 4. TGA mass loss curves of cured epoxides/HHMPA mixtures at a heating rate of 10 °C/min.

observed that thermosets from **5c** had a mass loss over a wider temperature range than **5e**, the secondary epoxide (**5a**), or the tertiary epoxide (**5b**) (see Figure 4). We believe that this behavior is due to the effect of the additional tertiary ester formed during curing. To examine this effect in greater detail, we synthesized the symmetric α-*terp*-epoxide (**5d**), which formed two tertiary esters during curing in addition to two linking tertiary esters. From Figure 4, we can clearly see in TGA measurements that thermosets from **5d**, while having a more pronounced weight loss than those from **5c**, have a slope almost equal to those curves from **5a**, **5b**, and **5e**.

To explain the differences observed with thermosets from **5b**, **5c**, and **5d**, we can consider the effect of acid generated by the thermal cleavage of the tertiary esters. For these three thermosets, the network starts to decompose at ~220 °C due to cleavage of tertiary esters. As well as causing additional ester cleavage, generated acid may be neutralized by trace volatile environmental organic base which can inhibit the acid catalysis of network breakdown. Such effects have been identified in the photoresist industry in similar chemical systems.[12] With increasing temperature, the acid groups may dehydrate to acid anhydride, which also decreases the effective acid concentration. At low temperature, the large fragments generated from β-scission are not volatile and the observed weight loss can be retarded. When the temperature is very high, the entire network starts to fragment, and in our experiments, the decomposition curve is indeed very sharp above 300 °C.

For the reworkable thermosets from **5c**, an additional weak linkage was built into the network. Even though the decomposition onset temperature was also around 220 °C, more acid was generated during the initial decomposition than in **5b**. Extra acid may lead to network breakdown at lower temperature, thus broadening the decomposition curve. The thermosets from symmetric α-*terp*-epoxides (**5d**) were designed to have even more weak linkages after curing. Unlike the other two thermosets with tertiary esters (**5b** and **5c**), when the initial decomposition temperature of **5d** is reached, a higher concentration of tertiary esters generates acid effectively over the entire network. In addition, the thermoset from **5d** has a lower glass transition temperature (100 °C, measured from TMA) compared to that for **5c** (140 °C, from TMA). Both tertiary ester concentration and T_g affect generation of acid and its diffusion in the network. These acids will efficiently attack additional esters to decompose the whole network even at lower temperatures.

Thermosets from **5d** show the same decomposition rate as thermosets from **5a**, **5b**, and **5e**, while the whole TGA curve is shifted to lower temperature. From a TGA study of cured mixtures of **5c** and **5e** with HHPA mixed in different ratios, we could observe a cooperative effect due to the acid generated from the **5c** tertiary ester. We note that while T_g plays some role in the efficiency of network cleavage, rework largely depends on tertiary ester concentration. From isothermal TGA data (Figure 5), a significant difference between thermosets could be observed. Thermosets from either **5e** or **5a** cured with HHMPA are stable to at least 230 °C, while at 230 °C thermosets from **5b** lose 7 wt % and those from **5c** lose more than 47 wt % after ~200 min. At 188 °C, similar effects are seen where the loss for thermosets from **5b** is 5 wt % and that from **5c** is 15 wt % after ~200 min. Again, we can see that the concentration of tertiary esters in the network will greatly affect the thermal decomposition behavior.

Reaction rate (R) may be expressed as the change in conversion (α) as a function of time (t) and related to an overall activation energy (E) as:

$$\ln R = \ln (d\alpha/dt) = F + \ln A - E/RT$$

where F is a constant and A is the preexponential factor.[13] From isothermal TGA data, at each measured conversion, α, we can plot ln (dα/dt) vs $1/T$, and the slope is $-E/R$, independent of the reaction order, n. At different degrees of conversion and temperature, the decomposition kinetics may be different and can be influenced by factors such as sample shape, volatility, thermal transfer, and local atmosphere. We therefore compared all samples under the same TGA conditions. The activation energy of the thermal decomposition as calculated above is the average activation energy at low conversion, $\alpha = 0.1-0.5$ (Table 1), which is due to the initial decomposition of the weak linkages. The resulting values have the same trends as seen from bond energies calculated using MOPAC. Thermosets with primary and secondary esters had much higher activation energies than thermosets with tertiary ester linkages. Although thermosets from α-*terp*-epoxide (**5c**) had different isothermal TGA curves than the tertiary epoxide (**5b**), they showed similar activation energies.

As we know, TGA can only measure the weight loss of the sample, which depends on sample volatility as

(12) MacDonald, S. A.; Hinsberg, W. D.; Wendt, H. R.; Clecak, N. J.; Willson, C. G. *Chem. Mater.* **1993**, *5*, 348.

(13) Schneider, H. A. In *Degradation and Stabilization of Polymers*; Jellinek, H. H. G., Ed.; Elsevier: New York, 1983; Vol. 1, p 506.

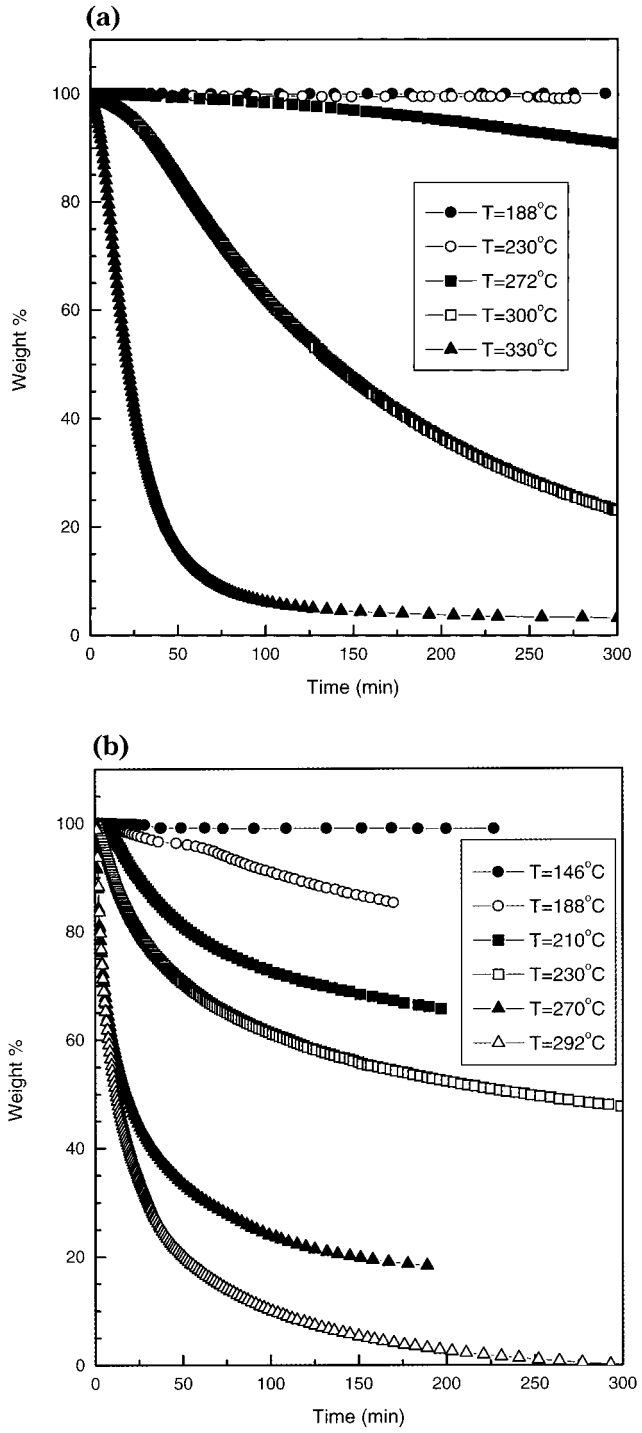

Figure 5. 5. (a) Isothermal TGA measurements of (**5e**)/HHMPA at different temperatures. (b) Isothermal TGA of (**5c**)/HHMPA at different temperatures.

well as decomposition mechanism. At a low temperature, the network may have already partially broken down, and the physical properties may have been changed even though the products are not volatile enough to produce any detectable mass change. As a result, TGA study was combined with other methods of thermal analysis to further investigate the decomposition mechanism.

Time-resolved FT-IR showed that when the cured thermosets (**5b**)/HHMPA, (**5c**)/HHMPA, and (**5d**)/HHMPA were heated to their thermal decomposition temperatures, absorbance bands at 1790, 988 (both acid anhydride), and 911 cm^{-1} (alkene, ν_{C-H}) developed, while the absorbance bands at 1730 (ester, $\nu_{C=O}$) and 1377 (CH_3, ν_{C-H}) cm^{-1} decreased. This observation is consistent with the ester thermal decomposition mechanism. The appearance of an acid anhydride peak is due to acid dehydration at high temperatures. This effect can be seen in Figure 6, in which (**5b**)/HHMPA was decomposed isothermally at 230 °C. Also shown in Figures 7 and 8, the absorbance changes at 1377 and 1730 cm^{-1} of different thermosets were followed from 30 to 300 °C, at a heating rate of 10 °C/min. Although there were baseline or film thickness changes which would affect the absorbance, (**5b**)/HHMPA and (**5c**)/HHMPA showed the same decomposition onset temperature, 240 °C, while (**5e**)HHMPA seemed to have no significant change up to 300 °C. These results are comparable to the data obtained from TGA (see Figure 3). *sym*-α-*terp*-epoxide (**5d**)/HHMPA showed quite different behavior. The thermoset started to decompose around 110 °C, which we believe was due to the higher concentration of tertiary esters in the cured network. We also note that the absorbance at 1730 cm^{-1} increased when decomposition started, and then dropped. We believe this was due to a change of the film thickness and transparency when acid and alkene were generated. Compared to TGA, FT-IR is more sensitive to changes of decomposition mechanism. All the above results suggest that we can cleave the thermoset networks at modest temperatures, which are above the processing temperature of the thermosets, without the need for any added solvent or catalyst.

Mechanical Properties. The reworkable thermosets were designed to retain the mechanical properties of conventional thermosets below the rework temperature. Thus mechanical properties above and below T_g are important issues for these reworkable thermosets, since these properties strongly depend on the extent of cross-linking. At their glass transition temperature (T_g), the polymer networks change from a glassy to a rubbery state accompanied by a modulus drop of 1 to 2 orders of magnitude. There will be a large increase of mobility of both the backbone and the side groups and a resulting drop in T_g with decreased cross-linking density.

As an example, the behavior of (**5c**)/HHMPA thermoset is described. A summary of mechanical properties is given in Table 2. From dynamic mechanical spectroscopy (DMS), it was found that the (**5c**)/HHMPA networks had a T_g around 160 °C, lower than that of (**5e**)/HHMPA, 190 °C. Below T_g, (**5c**)/HHMPA networks had a tensile modulus of ~5.5 GPa, comparable to that of (**5e**)/HHMPA, also 5.5 GPa. Above T_g, the tensile modulus of both the (**5c**)/HHMPA networks and the (**5e**)/HHMPA networks were still very similar (~180 MPa). The cross-linking density (ρ) can be calculated using the formula[5b]

$$E' = 3\rho RT = 3dRT/M_c$$

where E' is the tensile modulus at $T_g + 40$ °C, d is the sample density, M_c is the molecular weight between cross-links, R is the gas constant, and T is the absolute temperature at $T_g + 40$ °C.

The initial cross-linking densities were found to be 13.3 and 12.5 mol/kg for (**5c**)/HHMPA and (**5e**)/HHMPA,

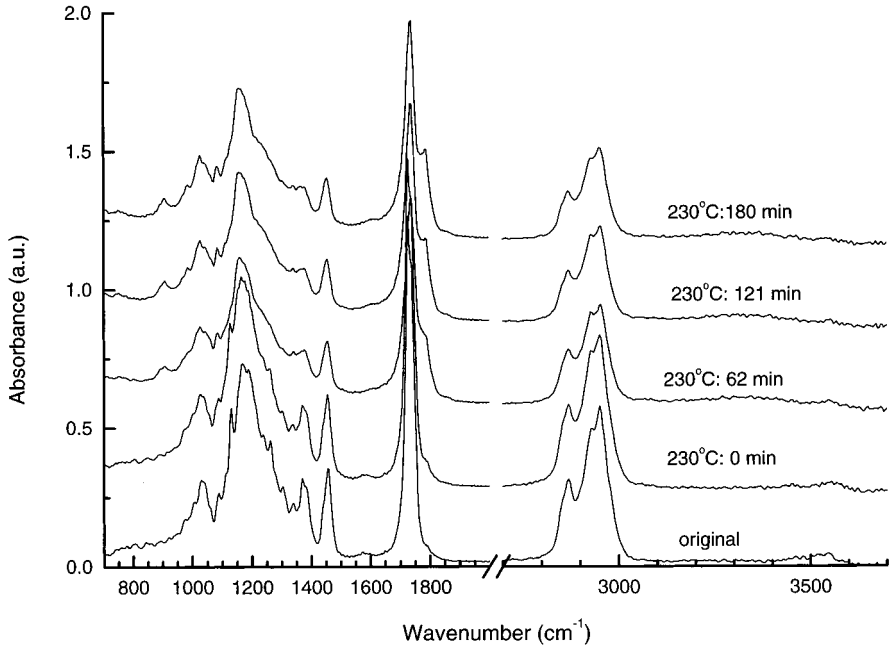

Figure 6. Time-resolved FT-IR of (**5c**)/HHMPA decomposed isothermally at 230 °C.

Table 1. Thermal Decomposition Activation Energies Calculated from Isothermal TGA Data

epoxide	activation energy E_a (kJ/mol)
ERL-4221 (**5e**)	186
secondary epoxide (**5a**)	183
tertiary epoxide (**5b**)	104
α-terp epoxide (**5c**)	102

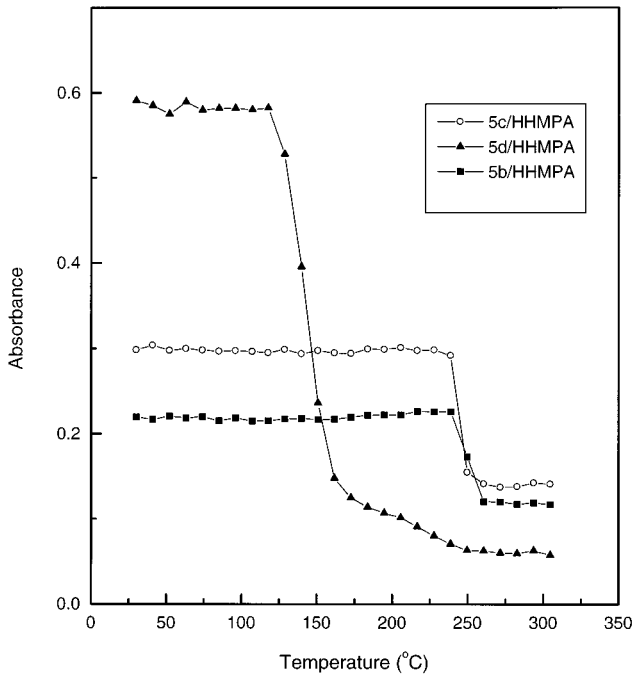

Figure 7. FT-IR absorbance at 1377 cm^{-1} monitoring decomposition of selected thermosets at a heating rate of 10 °C/min.

respectively. From dynamic mechanical analysis (DMA) in 3-point bending mode, the respective flexural moduli of (**5c**)/HHMPA and (**5e**)/HHMPA below T_g were ∼1.8 and ∼1.5 GPa. Above T_g, the flexural modulus of (**5e**)/HHMPA was ∼60 MPa. For the α-*terp*-epoxide/HHMPA, the test specimen softened to a state such that the flexural modulus could no longer be determined

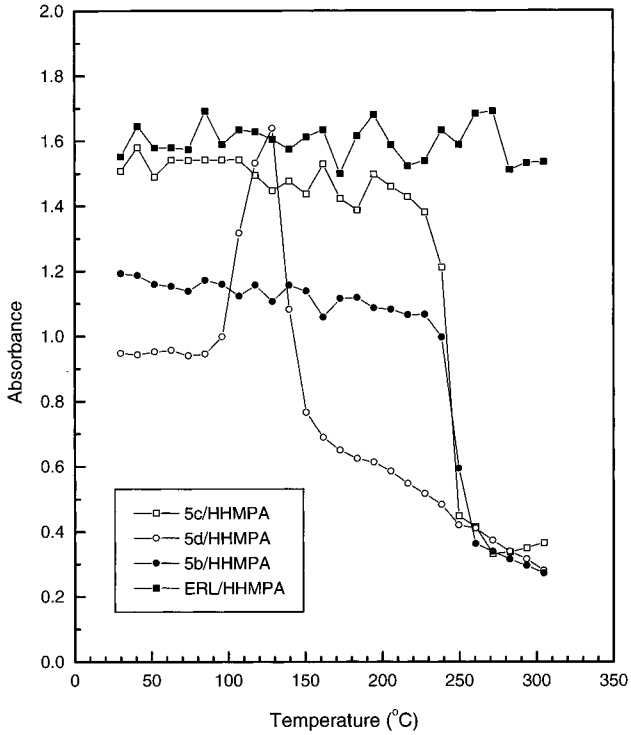

Figure 8. FT-IR absorbance at 1730 cm^{-1} monitoring decomposition of selected thermosets at a heating rate of 10 °C/min.

Table 2. Physical Properties of the Reworkable Thermosets (Cured with HHMPA)

sample	T_g[a] (°C)	tensile/flexural modulus (MPa) below T_g	tensile/flexural modulus (MPa) above T_g	CTE ($\times 10^6$ °C^{-1}) below T_g	ρ (mol/kg)
α-terp-epoxide (**5c**)	160	5500/1800	180/60	62	13.3
ERL-4221 (**5e**)	190	5500/1500	180/≤10	67	12.5

[a] T_g measured using DMS.

accurately (≲10 MPa). Given similar extents of initial cure, this means that the α-*terp*-epoxide (**5c**)/HHMPA is much weaker (more compliant) above T_g due to

network breakdown if heated above the rework temperature. Under isothermal conditions of T_g + 20 °C, (**5e**)/HHMPA maintained a constant tensile modulus of ~180 MPa for the entire testing duration of 12 h. Under identical conditions, (**5c**)/HHMPA maintained a constant tensile modulus of ~180 MPa for about 80 min, at which time the sample broke in a brittle manner. When the testing temperature was raised to T_g + 30 °C, the modulus of (**5e**)/HHMPA remained stable at ~180 MPa for 12 h, whereas (**5c**)/HHMPA only maintained its modulus of ~180 MPa for about 6 min before breaking in a brittle manner. From these initial studies, we believe the fracturing of the (**5c**)/HHMPA samples is due to embrittlement caused by the generation of acid within the (**5c**)/HHMPA system. The autoaccelerated breakdown of the (**5c**)/HHMPA network via acid generation thus makes it a favorable material for rework applications.

Conclusions

A series of epoxies with primary, secondary, and tertiary ester linkages were synthesized. Those networks which have tertiary esters break down at much lower temperatures (~220 °C) than those with primary or secondary esters. The thermosets cured from these epoxides have the advantage of being thermally decomposable at relatively modest temperatures without introduction of solvent or catalyst into the system. The concentration of weak linkages in the network greatly affects their decomposition behavior. The cured thermosets with tertiary esters retain the advantage of the mechanical behavior of conventional primary ester thermosets at room temperature while having reduced mechanical properties at elevated temperatures, thereby offering the possibility of easier thermoset removal.

Experimental Section

Chemicals. Most solvents and reagents were obtained from Aldrich and Fisher and were used without further purification.

Secondary Alcohol (1).[14] 1,2,3,6-Tetrahydrobenzaldehyde (15 g, 0.14 mol) was dissolved in anhydrous tetrahydrofuran and added to 60 mL of 3.0 M (0.18 mol) methylmagnesium chloride in THF. After addition, the mixture was refluxed for ~12 h, and 50 g of ice was added to hydrolyze the magnesium complex. The magnesium bromide precipitate was dissolved by 2 N hydrochloric acid. The organic phase was separated, washed with saturated sodium bisulfite and bicarbonate solution, and then dried over magnesium sulfate ($MgSO_4$). After fractional distillation, the yield was 12.0 g (70%). ^{1}H NMR ($CDCl_3$): δ 1.18−1.22 (dd, 3H, C*H*$_3$), 1.25−2.30 (m, 8H, ring C*H*, C*H*$_2$, O*H*), 3.62 (o, 1H, OC*H*), 5.68 (t, 2H, =C*H*). IR (film) 3385 cm^{-1} (OH), 1655 cm^{-1} (C=C).

Tertiary Alcohol (2).[15] Under N_2, 30 g (0.208 mol) of 3-cyclohexene acid chloride in 60 mL of anhydrous diethyl ether was slowly added to a 1000-mL three-neck round-bottom flask with 200 mL of 3.0 M methylmagnesium bromide in diethyl ether (0.60 mol) at about 0−5 °C. Then the mixture was refluxed in an oil bath for 2−3 h. After the solution had cooled in an ice bath, magnesium complex was decomposed by slowly adding cold saturated ammonium chloride solution through a separatory funnel. The organic phase was separated, and the aqueous phase was extracted with ether. Then the combined ether solution was washed with sodium bicarbonate and saturated sodium chloride solutions and dried over $MgSO_4$ with a yield of 18.2 g (57.7%) after fractional distillation. ^{1}H NMR ($CDCl_3$): δ 1.19 (d, 6H, C*H*$_3$), 1.2−1.35 (m, 2H, ring C*H*$_2$), 1.45−1.70 (m, 1H, ring C*H*), 1.75−2.25 (m, 5H, ring C*H*$_2$, O*H*), 5.68 (t, 1H, =C*H*), 5.69 (t, 1H, =C*H*). IR (film) 3387 (O−H), 1655 (C=C), 1377 cm^{-1} (doublet, C(CH$_3$)$_2$).

Acid Chloride Syntheses (3a−3b).[16] As an example, 60 g (0.46 mol) of anhydrous 3-cyclohexenecarboxylic acid (or 1,4-cyclohexanedicarboxylic acid, Lancaster) was placed in a 500-mL round-bottom flask. Under stirring, 1 or 2 drops of *N*,*N*-dimethylformamide (DMF) was added as a catalyst. Anhydrous toluene (49.1 mL, 0.46 mol) was then added with 1 molar ratio of excess thionyl chloride to drive off subsequent thionyl chloride. Thionyl chloride (67.3 mL, 0.92 mol) was introduced dropwise at room temperature, and the mixture was then refluxed for 4 h. The final product was fractionally distilled with a yield of 3-cyclohexene acid chloride (**3a**) of 55.32 g (83%). **3a**: ^{1}H NMR ($CDCl_3$): δ 1.7−2.7 (m, 6H, ring C*H*$_2$), 3.05 (m, ring *H*CCOCl), 5.76 (t, 1H, =C*H*), 5.64 (t, 1H, =C*H*). IR (film) 1798 (acid chloride C=O), 1655 cm^{-1} (C=C).

Esters Syntheses (4a−4d).[17,18] α-Terpineol (16.79 g, 0.109 mol) was dissolved in 15 mL (0.185mol) of anhydrous pyridine. Cooled in an ice−water bath, a solution of 15 g (0.104 mol) of 3-cyclohexenecarbonyl chloride in 50 mL of anhydrous methylene chloride was added slowly to the reaction flask with 1.268 g (0.0103 mol) 4-(dimethylamino)pyridine (DMAP) added as a catalyst. The mixture was stirred at room temperature overnight and then washed with 2 N HCl until all pyridine/HCl salt dissolved. The organic phase was separated, washed with saturated sodium bicarbonate and sodium chloride solution, and then dried over $MgSO_4$. The desired ester was purified by column chromatography with a yield of 16.36 g (60%) of **4c**. ^{1}H NMR (CDCl3) **4a** (secondary ester): δ 1.18−1.22 (dd, 3H, C*H*$_3$), 1.25−2.40 (m, 13H, ring C*H*, C*H*$_2$), 2.4−2.7 (m, 1H, ring *H*CCOO), 4.85 (o, 1H, secondary *H*COOC), 5.68 (t, 4H, =C*H*); **4b** (tertiary ester): δ 1.46 (d, 6H, 2C*H*$_3$), 1.2−2.35 (m, 13H, ring C*H*, C*H*$_2$), 2.48−2.58 (m, 1H, ring *H*CCOO), 5.68 (t, 4H, =C*H*); **4c** (α-*terp*-ester): δ 1.37−1.40 (d, 6H, 2C*H*$_3$), 1.59 (s, 3H, C*H*$_3$), 1.49−2.17 (m, 13H, ring C*H*, C*H*$_2$), 2.39 (m, 1H, ring *H*CCOO), 5.32 (s, 1H, =C*H*), 5.62 (s, 2H, =C*H*); **4d** (*sym*-α-*terp*-ester): δ 1.3−2.21 (m, 22H, ring C*H*, C*H*$_2$), 1.45 (d, 12H, 4C*H*$_3$), 1.65 (s, 6H, 2C*H*$_3$), 2.30−2.48 (m, 2H, ring *H*CCOO), 5.38 (s, 2H, =C*H*). IR (film) **4a**: 1728 (ester C=O), 1655 cm^{-1} (C=C); **4b**: 1730 (ester C=O), 1655 cm^{-1} (C=C); **4c**: 1726 (ester C=O), 1655 (C=C), 1439, 1375 cm^{-1} (C(CH$_3$)$_2$); **4d**: 1725 (ester C=O), 1655 (C=C), 1450, 1375 cm^{-1} (C(CH$_3$)$_2$).

Epoxides Syntheses (5a−5d).[19,20] OXONE, monopersulfate compound ($2KHSO_5 \cdot KHSO_4 \cdot K_2SO_4$) (11.71 g, 19.05 mmol), in 60 mL of 4 × 10^{-4} M aqueous disodium EDTA was added dropwise to a stirred biphasic mixture of 1 g (3.81 mmol) of

(14) Furniss, B. S.; Hannaford, A. J.; Smith, P. W. G.; Tatchell, A. R. *VOGEL's Textbook of Practical Organic Chemistry*, 5th ed.; Wiley: New York, 1989; p 537, expt. 5.40.

(15) (a) Furniss, B. S.; Hannaford, A. J.; Smith, P. W. G.; Tatchell, A. R. *VOGEL's Textbook of Practical Organic Chemistry*, 5th ed.; Wiley: New York, 1989; p 541, expt. 5.42. (b) Larock, R. C. *Comprehensive Organic Transformations*; VCH Publishers: New York, 1989; p 559.

(16) Furniss, B. S.; Hannaford, A. J.; Smith, P. W. G.; Tatchell, A. R. *VOGEL's Textbook of Practical Organic Chemistry*, 5th ed.; Wiley: New York, 1989; p 693, expt. 5.138.

(17) Steglich, W.; Hrfle, G. *Angew. Chem., Int. Ed. Engl.* **1969**, *8*, 981.

(18) IUPAC names: **4a**, cyclohex-3-enecarboxylic acid 1-cyclohex-3-enylethyl ester; **4b**, cyclohex-3-enecarboxylic acid 1-cyclohex-3-enyl-1-methylethyl ester; **4c**, cyclohex-3-enecarboxylic acid 1-methyl-1-(4-methylcyclohex-3-enyl)ethyl ester; **4d**, cyclohexane-1, 4-dicarboxylic acid bis[1-methyl-1-(4-methylcyclohex-3-enyl)ethyl] ester.

(19) Curci, R.; Fiorentino, M.; Troisi, L. *J. Org. Chem.* **1980**, *45*, 4758−4760.

(20) IUPAC names: **5a**, 7-oxabicyclo[4.1.0]heptane-3-carboxylic acid 1-(7-oxabicyclo[4.1.0]hept-3-yl)ethyl ester; **5b**, 7-oxabicyclo[4.1.0]-heptane-3-carboxylic acid 1-methyl-(7-oxabicyclo[4.1.0]hept-3-yl)ethyl ester; **5c**, 7-oxabicyclo[4.1.0]heptane-3-carboxylic acid 1-methyl-1-(6-methyl-7-oxabicyclo[4.1.0]hept-3-yl)ethyl ester; **5d**, cyclohexane-1,4-dicarboxylic acid bis[1-methyl-1-(6-methyl-7-oxabicyclo[4.1.0]hept-3-yl)ethyl] ester; **5e** (**ERL-4221**), 7-oxabicyclo[4.1.0]heptane-3-carboxylic acid 7-oxabicyclo[4.1.0]hept-3-ylmethyl ester.

ester **4c**, 50 mL of methylene chloride, 5 mL (68 mmol) of acetone, and 100 mL of buffer (pH 8.0). During addition, the reaction temperature was kept at 0−5 °C by using an ice−water bath. 18-Crown-6 ether (0.20 g, 0.76 mmol) was used as a phase-transfer catalyst. During the reaction, the pH was maintained at ∼7−7.5 by adding sodium bicarbonate solution. After ∼12 h, the organic layer was removed and the aqueous layer was extracted with methylene chloride. The combined organic layers were washed with saturated $NaHCO_3$ and NaCl solution and then dried over $MgSO_4$. Finally, the epoxy was purified by flush column chromatography with a yield of **5c** of 0.97 g (86.7%). ^{1}H NMR (CDCl3) **5a**: δ 1.11−1.16 (d, 3H, CH_3), 1.2−2.3 (m, 13H, ring CH, CH_2), 2.5 (m, 1H, ring HCCOO), 3.15−3.25 (dd, 4H, epoxy HCOC), 4.71 (o, secondary HCOOC); **5b**: δ 1.35−1.48 (dd, 6H, 2CH_3), 1.2−2.3 (m, 13H, ring CH, CH_2), 2.4 (m, 1H, HCCOO), 3.1−3.3 (d, 4H, epoxy HCOC); **5c**: δ 1.3 (d, 3H, CH_3), 1.37−1.40 (d, 6H, 2CH_3), 1.2−2.3 (m, 13H, ring CH, CH_2), 2.4 (m, 1H, HCCOO), 2.97 (d, 1H, epoxy HCOC), 3.1−3.2 (t, 2H, epoxy HCOC); **5d**: δ 1.3−2.21 (m, 22H, ring CH, CH_2), 1.31 (dd, 6H, 2CH_3), 1.41 (dd, 12H, 4CH_3), 2.15−2.35 (m, 2H, ring HCCOO), 2.98−3.0 (d, 1H, epoxy HCOC), 3.06 (s, 1H, epoxy HCOC). IR (film) **5a**: 1726 (ester C═O), 1254, 860, 797 cm^{-1}, (epoxy C−C−O); **5b**: 1726 (ester C═O), 1254, 905, 860, 797 cm^{-1} (epoxy C−C−O); **5c**: 1724 (ester C═O), 1438, 1377 (C(CH_3)$_2$), 1254, 916, 883,843, 797 cm^{-1} (epoxy C−C−O); **5d**: 1725 (ester C═O), 1455, 1375 (C(CH_3)$_2$), 1250, 885, 760 cm^{-1} (epoxy C−C−O).

Curing Reactions. The diepoxides were cured with either hexahydro-4-methylphthalic anhydride (HHMPA) or *cis*-1,2-cyclohexanedicarboxylic anhydride (HHPA) as hardener, ethylene glycol as initiator, and benzyldimethylamine (BDMA) as catalyst.[9] Samples used for TGA measurement were cured on a digital hotplate at 100 °C for 1 h and then at 145 °C (160 °C for ERL-4221) for 2−3 h. Samples for DMA and DMS measurements were degassed in the mold under vacuum at room temperature, precured at 90−100 °C for 1 h and then cured at 140−145 °C for 4 h (160 °C for ERL-4221) not in a vacuum, and then cooled slowly.

The curing reactions were studied by differential scanning calorimetry (DSC) and time-resolved FT-IR in the range of 100−180 °C. The DSC measurements were carried out under dry nitrogen flow with a Perkin-Elmer DSC-7 series. Aluminum volatile sample pans and covers were chosen for the curing. Cure time was determined by DSC following the method described by Sourour and Kamal,[21] which involved preheating the DSC to the preset temperature and then inserting the sample pan into the cell as quickly as possible. For time-resolved FT-IR measurements,[10] a thin film of mixtures was cast between two sodium chloride windows on the Mettler hot stage (FP82HT), which was then mounted into a Mattson 2020 Galaxy Series FT-IR spectrometer. The resolution was 4 cm^{-1}.

Characterization. The decomposition temperature of the thermosets was determined by means of a TA Instruments thermogravimetric analyzer (TGA) 951 under nitrogen flow. The decomposition mechanism was studied by time-resolved FT-IR as described above. The tensile modulus and glass transition temperature (T_g) of the thermosets were measured on a Seiko Instruments dynamic mechanical spectrometer (DMS) at a heating rate of 2 °C/min. The flexural modulus was determined by a Perkin-Elmer dynamic mechanical analyzer (DMA)-7 in 3-point bending mode at a heating rate of 2 °C/min. The coefficient of thermal expansion and T_g were measured by a TA Instruments thermomechanical analyzer (TMA) 943 at a cooling rate of 5 °C/min.

Bond Energy Calculation. The ester bond energy of the epoxies was estimated using a MOPAC ver. 6.0 programmed by J. J. P. Stewart. Keywords of PM3, UHF, PRECISE, and GNORM were used for calculations.

Acknowledgment. Financial support from IBM Microelectronics (S.Y.), the Industry−Cornell University Alliance for Electronic Packaging, and Hoechst and DAAD for support of T.B. are gratefully acknowledged. We also thank the Wright Materials Laboratories for support for H.K. Finally, A. Shiota (JSR) is thanked for his kind help and many useful discussions.

Registry Nos. (Supplied by Author): 1,4-cyclohexanedicarboxylic acid, 1076-97-7; *cis*-1,2-cyclohexanedicarboxylic anhydride, 13149-00-3; 3-cyclohexenecarboxylic acid, 4771-80-6; ERL-4221(3,4-epoxycyclohexylmethyl 3,4-epoxycyclohexanecarboxylate), 2386-87-0; hexahydro-4-methylphthalic anhydride, 19438-60-9; $KHSO_5$, 10058-23-8; OXONE, 37222-66-5.

CM970667T

(21) Sourour, S.; Kamal, M. R. *Thermochim. Acta* **1976**, *14*, 41.